

Remote Detection of Quaternary Borate Deposits with ASTER Satellite Imagery as a Geothermal Exploration Tool

Chris Kratt¹, Mark Coolbaugh², and Wendy Calvin²

¹Desert Research Institute, Reno, NV

²Arthur Brant Laboratory for Exploration Geophysics and the Great Basin Center for Geothermal Energy, University of Nevada, Reno, NV

Keywords

Borates, remote sensing, ASTER, Nevada, geothermal, spectroscopy, Rhodes, Teels, Columbus

ABSTRACT

In the Great Basin of the western United States, geothermal fluids are sometimes associated with surface crusts of borate evaporite minerals. These borates can therefore potentially serve as a geothermal exploration tool if they can be efficiently identified and mapped in the field. We demonstrate the effectiveness of using a field-portable ASD Fieldspec[®] spectroradiometer, and satellite-based Advanced Spaceborne Thermal and Emitted Reflectance Radiometer (ASTER) imagery for mapping borate minerals in the field. Using the ASTER imagery reflectance characteristics of tinalconite in the 0.4-2.5 μm wavelength region as a guide, remotely generated mineral abundance maps were made for Rhodes, Teels, and Columbus Marshes (playas), located in western Nevada. Field observations confirmed the presence of borate evaporite crusts in each of these locations and chemical analyses of well, spring and groundwater samples suggest the possible presence of hidden subsurface geothermal reservoirs. Cation and quartz geothermometer analyses yield reservoir temperature estimates between 118° C and 162° C at all three areas where waters were sampled in close proximity to borax and tinalconite evaporite crusts.

Introduction

The high reflectance characteristics of borate minerals make them ideal for detection with remote sensing methods where they occur as playa deposits or hot spring aprons produced by evaporation of geothermal fluids. Borate deposits and geothermal activity typically occur in active tectonic settings characterized by magmatism and faulting. It has long been recognized that many Quaternary borate deposits form from boron-rich thermal waters. These waters may have acquired

their boron by leaching country rock, or from contributions from magmatic fluids. Examples of regions where major borax deposits are found include the western United States, Turkey, China, Nepal, India, and the Puna Region of the Andes mountains (Garrett, 1998; Barker and Lefond, 1985).

There are several genetic models for Quaternary surface borate deposits but they all require extensive evaporation rates, given that fact that most borate minerals are highly soluble in water (Barker and Lefond, 1985). These models explain the formation of borate minerals in: 1) spring aprons; 2) ephemeral saline lakes and playas; and 3) perennial saline lakes. In spring apron deposits borates form as an apron of efflorescent crust adjacent to thermal springs in the downslope direction. In ephemeral saline lakes or playas borate crusts can form from short-lived brines on playa surfaces or from the evaporation of saline groundwaters by capillary action. In that latter case, crystallization occurs during daytime evaporation in the summer months and in winter crystallization occurs by cooling of the surface brine (Garrett, 1998). Perennial saline lakes are responsible for the largest borate deposits, which form near the bottom of perennial lakes that are fed by thermal springs, such as those formed at Furnace Creek (Barker and Lefond, 1985).

During the 1800s, hot springs were used as a guide for borate exploration in Nevada (Barker and Lefond, 1985). However, prior to the current research there were at least three places known in Nevada where playa borate deposits are associated with what are considered to be blind geothermal systems (Salt Wells, Fish Lake Valley, and Soda Lake). In these areas surface hot springs are either non-existent or minimally expressed (Coolbaugh et al., 2006a). We present evidence here that additional occurrences of borates associated with blind geothermal systems may exist in the Great Basin.

Remote sensing spectroscopy provides an efficient means for locating borate minerals on seemingly homogenous and areally extensive playa surfaces. To the unaided eye the more common borate minerals have the same general appearance as many other evaporate minerals. However, spectral measurements of visible, near-infrared, and short-wave infrared (0.4-2.5

μm) solar reflected energy reveal unique spectral characteristics of the borates that distinguish them from other evaporite minerals and allow them to be systematically mapped. We analyzed both field and satellite remote sensing data to identify and map borates in playas where they have been reported to occur, but where no previous detailed maps of borate mineralization existed. Spring and groundwater samples were then taken proximal to areas of borate mineralization and geochemically analyzed to assess the potential for subsurface geothermal activity (Coolbaugh et al., 2006a).

Study Area Background

An initial orientation survey testing the remote sensing methods was performed in the Salt Wells area in Churchill County, Nevada. During a three-year period at Salt Wells beginning in 1870, the American Borax Company produced 23.5 tons of borax from surface evaporite deposits covering a 400-acre portion of the 32-km² playa (Garrett, 1998). A large, blind geothermal system occurs in the subsurface (e.g. Klein et al., 2004). Subtle surface indicators of subsurface geothermal activity include silicified sediments, siliceous sinter, argillic alteration, ephemeral hot and warm springs/seeps, and anomalous shallow ground temperatures (Coolbaugh et al., 2006b). Thermal fluids from wells and seeps at Salt Wells contain 9-14 ppm B and are believed to be responsible for the formation of surface borate mineralization.

After the initial orientation survey, we investigated three other borate-bearing playas in Nevada in more detail, which are located at Teels, Rhodes and Columbus Marshes; these three playas are located in southwestern Nevada (Figure 1). Together with Fish Lake Marsh, also in the same region but not covered by the ASTER scene, these playas were the world's leading sources of mined borate minerals during the 1870s and

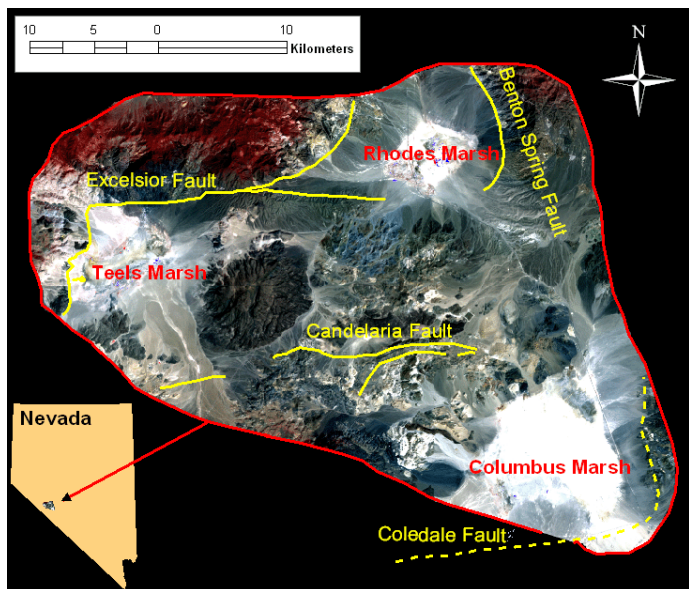


Figure 1. ASTER channel 3, 2, 1 composite showing study area with respect to location in Nevada. Major faults are shown in yellow (modified from Wesnousky (2005)).

lasting for about a decade (Barker and Lefond, 1985). With the exception of Fish Lake Marsh, none of these locations were previously known to host active geothermal systems. These playas formed in closed extensional basins within a broad right-stepping transfer zone in the Walker Lane. In this transfer zone, right-lateral strike-slip strain is transferred from the southern to the central Walker Lane Belt along a series of east-northeast-striking left-lateral faults that show evidence of Quaternary displacement (Wesnousky, 2005). Although they are all closed basins, boron weathered from the country rock does not by itself account for the high concentration of boron in the playas (Garrett, 1998).

Remote Sensing Background

Ground, airborne and spaceborne remote sensing spectroradiometers measure reflected solar energy in the visible/near infrared (VNIR) and short-wave infrared (SWIR) ranges (0.4 to 2.5 μm). These measurements take advantage of the interaction of light with both cations (Fe, Mg, Al) and anions (OH, H₂O, CO₃) in the mineral structure (Hunt, 1977). There are a limited number of publications on the detection of borates with remote sensing data. Crowley (1993) and Stearns and van der Horst (1999) report on mapping the well-exposed Tertiary borate deposits of the Furnace Creek area, Death Valley, CA with AVIRIS (Airborne Visible/Infrared Imaging Spectrometer) hyperspectral data. Utilizing the 224 narrow and contiguous channels in the 0.4-2.5 μm range they were able to produce mineral abundance maps for hydroboracite (CaMgB₆O₁₁·6H₂O), pinnoite (MgB₂O₄·3H₂O), (Na₆MgB₂₄O₄₀·22H₂O), colemanite (Ca₂B₆O₁₁·5H₂O) and ulexite (NaCaB₅O₆(OH)₆·5H₂O). Crowley et al. (2000) produced similar results with MODIS/ASTER Airborne Simulator (MASTER) data acquired over Furnace Creek. Khalalili and Safaei (2002) used Optimum Index Factor Landsat images to produce a thematic map of ulexite evaporite crusts in Iran.



Figure 2. ASD spectroradiometer deployed at Salt Wells. Tincalconite and halite both appear in the photo as efflorescent evaporite crusts.

We employed an Analytical Spectral Devices (ASD) spectroradiometer for in situ spectral measurements in the field. The ASD samples 2,151 spectral channels covering the VNIR and SWIR wavelengths of light. Reflectance calibration is achieved with a white reference panel that has a known reflectance across the entire measured spectrum. Real-time spectra are displayed on the computer screen when the optical detector is pointed at the ground from a distance of 0.05 – 1 meters (Figure 2). For Teels, Rhodes, and Columbus Marshes, we analyzed reflectance data from an ASTER scene acquired in August, 2003. The scene covers 60 by 60 km. Three channels record reflected radiance in the VNIR at 15 m spatial resolution, and six channels in the SWIR with 30 meter spatial resolution (Yamaguchi et al., 1998).

Methods

Hydroxyl ions and water molecules found in the structure of borate minerals cause strong absorption features that result in a first-order reflectance characteristic that can be used to generally distinguish them from more common playa evaporate minerals such as thenardite (NaSO_4), halite (NaCl), calcite (CaCO_3) and common clays (Crowley, 1991); borate spectra display a strong “cascade” effect where reflectance is very high in the VNIR and then dramatically decreases from about 1.4-1.9 μm and then decreases again between 2.0-2.5 μm (Figure 3). Although a few non-borate evaporite minerals display similar features, this characteristic is useful as a first-cut approach. A full, unique discrimination of borate minerals requires high-spectral-resolution data or a few well positioned multispectral channels that take advantage of narrow and less pronounced absorption features that are specific to borate minerals.

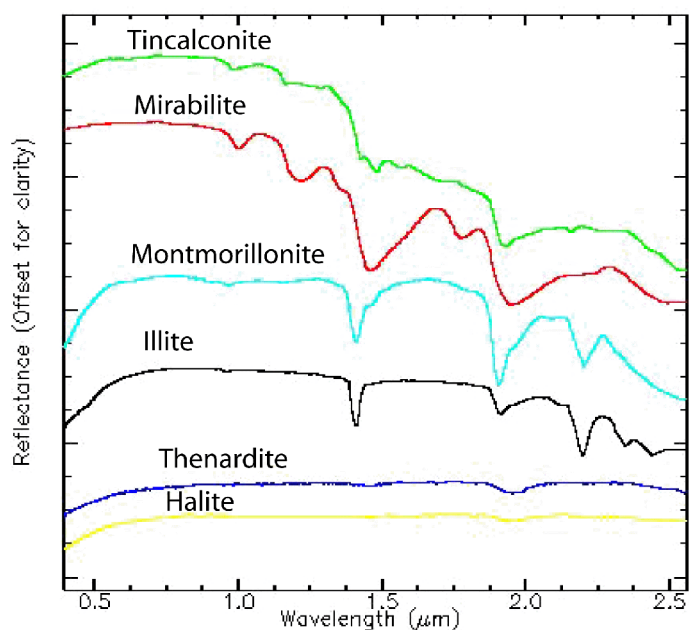


Figure 3. Tincalconite ($\text{Na}_2\text{B}_4\text{O}_5(\text{OH})_4 \cdot 3\text{H}_2\text{O}$) spectra compared with spectra of selected minerals that are common to playa surfaces. (USGS spectral library, Clark, et al., 2005).

An exploratory “wildcatting” ground traverse with the ASD was carried out at Salt Wells in the general area of borate crusts reported by Papke (1976). Real-time spectra on the computer display allowed the borate mineral tincalconite ($\text{Na}_2\text{B}_4\text{O}_5(\text{OH})_4 \cdot 3\text{H}_2\text{O}$) to be recognized by the tell-tale cascade effect and by specifically matching wavelength positions of narrow absorption features with evaporite mineral reference spectra from Crowley (1991). In order to predict how the tincalconite spectra would appear with the lower spectral resolution of ASTER satellite-based imagery, the tincalconite field spectra were smoothed (i.e. convolved) to the same spectral resolution as the ASTER VNIR and SWIR channels (Figure 4). This convolved spectra was then used to design a spectral unmixing algorithm discussed in the following paragraphs.

Prior to any spectral processing it was first convenient to combine the 15 m resolution VNIR data and the 30-m-resolution SWIR data into one file. This was achieved by resampling the 30 m SWIR channels to 15 m. We could then take advantage of reflectance characteristics in both the VNIR and SWIR when trying to match ASTER spectra to the convolved tincalconite spectra. The Mixture Tuned Matched Filtering (MTMF) approach was then used to identify ASTER image pixels that resembled the convolved tincalconite spectra. MTMF is a spectral unmixing algorithm that assumes linear mixing and uses a combination of matrix algebra, least squares fitting, and vectors in n-dimensional space, where n is equal to the number of spectral channels (Boardman et al., 1995). Goodness-of-fit was determined for each ASTER pixel spectra relative to the input spectra (tincalconite), after a mask was applied in order to limit processing to just the marshes (playas). Pixels indicated to have high match potential were combined with other spatial data in a Geographic Information System (GIS) and then field checked. Field observations were used to adjust a threshold value to the MTMF result before making a final borate abundance map.

Water from wells and springs near borate-bearing areas were sampled and chemically analyzed and geothermometer estimates of possible geothermal reservoir temperatures were calculated (Coolbaugh et al., 2006a). The mineralogy of evaporite samples was verified with laboratory spectral measurements and X-ray diffraction analyses.

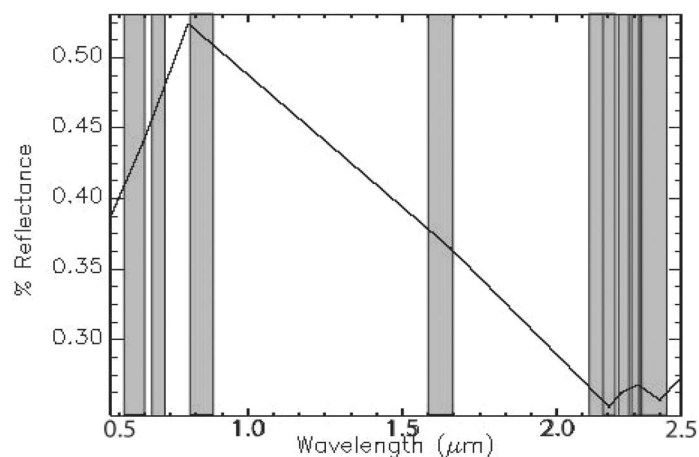


Figure 4. Field tincalconite spectra convolved to ASTER spectral resolution. Shaded areas show wavelengths covered by ASTER channels.

Results

The ASD Fieldspec® spectroradiometer was effective in re-locating the historic remains of the Salt Wells borate processing works at three different sites on the edge of the playa and recognizing evaporite distribution patterns on the playa (refer to Figure 2 of Coolbaugh et al., 2006b). Field spectra were essential for distinguishing tincalconite from nearby salt minerals (Figure 3). The borate crusts were in some cases up to 15 cm thick but typically less than about 8 cm. The top few centimeters were composed of tincalconite, the dehydrated version of borax, while the bottom portion of samples typically contained borax ($\text{Na}_2\text{B}_4\text{O}_5(\text{OH})_4 \cdot 8\text{H}_2\text{O}$). A close spatial relationship between borate occurrences and shallow zones of hot groundwater at Salt Wells suggests that the borate minerals are precipitating from upwelling geothermal fluids and evaporation by capillary action (Coolbaugh et al., 2006b).

The processed ASTER image was effective in mapping borate occurrences at each of Rhodes, Teels, and Columbus Marshes (Figure 5). Well, spring and groundwater geothermometer estimates from water samples taken at or near these

locations suggest the possible presence of geothermal reservoirs at depth in each of these basins. At Teels Marsh there was 209 mg/L of boron in groundwater sampled adjacent to borate crusts that have reformed in the area of historic borate mining. Warm artesian wells at Rhodes Marsh yielded 7 mg/L of boron nearest to the western and less contiguous borate crusts and 319 mg/L boron adjacent to the largest and most contiguous borate crusts to the east. At Columbus Marsh an isolated occurrence of borates were mapped in addition to borate crusts proximal to a cold spring that yielded 22 mg/L of boron. Coolbaugh et al. (2006a) gives a more detailed explanation of the geochemical data and analyses.

Conclusions and Future Work

The ASTER VNIR and SWIR channels were used to successfully map the distribution of borate evaporite crusts on three different playas in western Nevada. At each of these locations, evidence suggests a relationship between borates and geothermal fluids. Given the broad-area coverage of ASTER and minimal processing effort involved, we plan to apply the

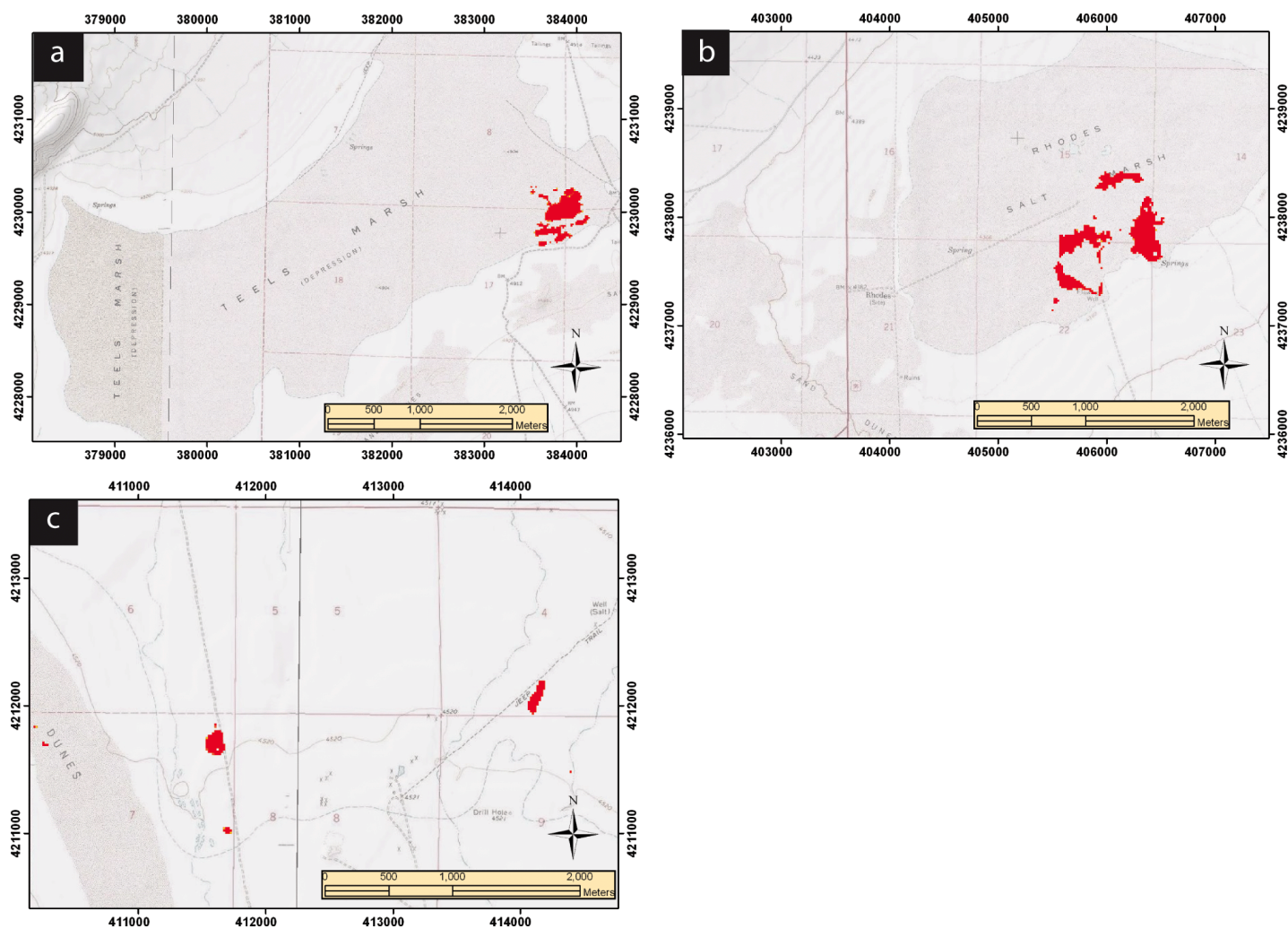


Figure 5. Tincalconite evaporite crusts (shown in red) mapped with ASTER data at: a) Teels Marsh; b) Rhodes Marsh; and c) Columbus Marsh.

same methodology to ASTER scenes that cover other playas in western Nevada. Any new borate occurrences identified with this remote sensing mapping has the potential to lead to the discovery of additional geothermal systems.

References

- Barker, J. M. and S. J. Lefond, 1984. Borates: economic geology and production. Proceedings of a Symposium at the fall meeting of SME-AIME, Denver, Colorado, October 24.
- Boardman, J. W., F. A. Kruse, and R. O. Green, 1995. Mapping Target Signatures Via Partial Unmixing of AVIRIS Data. Proceedings of the Fifth JPL Airborne Earth Science Workshop, JPL Publication 95-1 (1), p. 23-26.
- Coolbaugh, M.F., Kratt, C., Sladek, C., Zehner, R.E., and Shevenell, L., 2006a. Quaternary borate deposits as a geothermal exploration tool in the Great Basin: Geothermal Resources Council Transactions, (this volume).
- Coolbaugh, M.F., Sladek, C., Kratt, C., and Shevenell, L., 2006b. Surface indicators of geothermal activity at Salt Wells, Nevada, USA, including warm ground, borate deposits, and siliceous alteration: Geothermal Resources Council Transactions (this volume).
- Crowley, J. K., 1991. Visible and near-infrared (0.4-2.5 μm) reflectance spectra of playa evaporite minerals. *Journal of Geophysical Research*, v. 96, n. B10, p. 16,231-16,240.
- Crowley, J. K., 1993. Mapping playa evaporite minerals with AVIRIS data: a first report from Death Valley, California. *Remote Sensing of Environment*, v. 44, p. 337-356.
- Crowley, J. K., and S. B. Carpenter, 1999. Association of magnesium-rich clay minerals and borate deposits: a potential remote sensing guide for borate mineral exploration? Thirteenth International Conference on Applied Geologic Remote Sensing, Vancouver, British Columbia, Canada, 1-3 March.
- Crowley, J. K., J. C. Mars, and S. J. Hook, 2000. Mapping evaporite minerals in the Death Valley salt pan using MODIS/ASTER airborne simulator (MASTER) data. Presented at the Fourteenth International Conference on Applied Geologic Remote Sensing, Las Vegas, Nevada, 6-8 November.
- Garrett, D. E. 1998. Borates: Handbook of deposits, processing, properties, and use. Academic Press, New York.
- Hunt, G. H., 1977. Spectral signatures of particulate minerals in the visible and near-infrared. *Geophysics*, vol. 42, no. 3, pp. 501-513.
- Papke, K.G., 1976. Evaporites and brines in Nevada playas: Nevada Bureau of Mines and Geology Bulletin 87, pp. 35.
- Smith, G.I., 1976. Origin of lithium and other components in the Searles Lake evaporates, California, in Vine, J.D., ed., *Lithium Resources and Requirements by the Year 2000*: United States Geological Survey Professional Paper 1005, p. 92-103.
- Stearns, S. V., E. van der Horst, and G. Swihart, 1999. Hyperspectral mapping of borate minerals in Death Valley, California. Thirteenth International Conference on Applied Geologic Remote Sensing, Vancouver, British Columbia, Canada, 1-3 March.
- Wesnousky, S. G., 2005. Active faulting in the Walker Lane. *Tectonics*, v. 24, pp. 35.
- Yamaguchi, Y., A. B. Kahle, H. Tsu, T. Kawakami, and M. Pniel, 1998. Overview of Advanced Spaceborne Thermal Emission and Reflection Radiometer (ASTER). *IEEE Transactions on Geoscience and Remote Sensing*, v. 36, no. 4.

